Atmospheric Chemistry of Cyclohexane: UV Spectra of c-C_6H_{11}• and (c-C_6H_{11})O_2• Radicals, Kinetics of the Reactions of (c-C_6H_{11})O_2• Radicals with NO and NO_2, and the Fate of the Alkoxy Radical (c-C_6H_{11})O•

J. Platz, J. Sehested,[†] and O. J. Nielsen*[,‡]

Department of Atmospheric Chemistry Plant Biology and Biogeochemistry, Risø National Laboratory, DK-4000, Roskilde, Denmark

T. J. Wallington*[,§]

Ford Motor Company 20000 Rotunda Drive, Mail Drop SRL-3083, Dearborn, Michigan 48121-2053

Received: October 27, 1998; In Final Form: December 30, 1998

A pulse radiolysis technique was used to measure the UV absorption spectra of c-C_6H_{11}• and (c-C_6H_{11})O_2• radicals over the ranges 230−290 and 220−300 nm, σ(c-C_6H_{11}•)$_{250\ nm}$ = (7.0 ± 0.8) × 10^{-18} and σ((c-C_6H_{11})O_2•)$_{250\ nm}$ = (5.7 ± 0.6) × 10^{-18} cm^2 molecule^{-1}. The rate constant for the self-reaction of c-C_6H_{11}• radicals was k_3 = (3.0 ± 0.4) × 10^{-11} cm^3 molecule^{-1} s^{-1}. The addition reaction of c-C_6H_{11}• radicals with O_2 proceeds with a rate constant k_2 = (1.3 ± 0.2) × 10^{-11} cm^3 molecule^{-1} s^{-1}. Rate constants for reactions of (c-C_6H_{11})O_2• radicals with NO and NO_2 were k_4 = (6.7 ± 0.9) × 10^{-12} and k_5 = (9.5 ± 1.5) × 10^{-12} cm^3 molecule^{-1} s^{-1}, respectively. FTIR−smog chamber techniques were used to record the IR spectrum of the peroxynitrate (c-C_6H_{11})O_2NO_2, determine that the reaction between (c-C_6H_{11})O_2• radicals and NO produces a (16 ± 4)% yield of the nitrate (c-C_6H_{11})ONO_2, and study the atmospheric fate of cyclohexoxy radicals. Decomposition via C−C bond scission and reaction with O_2 are competing fates of the cyclohexoxy radical. In 700−750 Torr total pressure at 296 ± 2K, the rate constant ratio k_{decomp}/k_{O2} = (8.1 ± 1.5) × 10^{18} molecule cm^{-3}. At 296 K in 1 atm of air, 61% of cyclohexoxy radicals decompose and 39% react with O_2. These results are discussed with respect to the literature data concerning the atmospheric chemistry of cyclohexane and analogous compounds.

1. Introduction

Alkanes constitute a significant fraction of automotive fuels, vehicle emissions, and air pollution in urban areas. Atmospheric oxidation of alkanes is initiated primarily via attack by OH radicals giving alkyl radicals which then add O_2 to give alkyl peroxy radicals. Subsequent reactions of the alkyl peroxy radicals determine the atmospheric degradation mechanism, and hence ozone forming potential, of organic compounds. There are two reasons why we are interested in the atmospheric chemistry of cyclohexane. First, cyclohexane is present in small, but significant (0.1−1.0 wt %), amounts in typical gasoline blends sold in the U.S., Germany, and the U.K.[1] An understanding of the atmospheric chemistry of cyclohexane is needed to assess the impact of its release into the environment. Second, cyclohexane has a unique unstrained cyclic structure and information concerning the reactivity of the radicals generated during its oxidation provides insight into the likely behavior of analogous secondary radicals formed during the oxidation of other alkanes.

The atmospheric degradation of c-C_6H_{12} is initiated by reaction with OH radicals giving an alkyl radical which adds O_2 to form an alkyl peroxy radical:

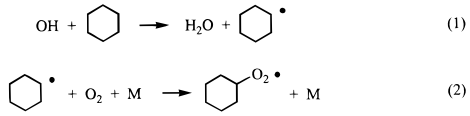

(1)

(2)

We have used pulse radiolysis coupled with time-resolved UV−vis absorption spectroscopy to determine the UV absorption spectra of the c-C_6H_{11}• and (c-C_6H_{11})O_2• radicals, and the kinetics of the reactions 2−5.

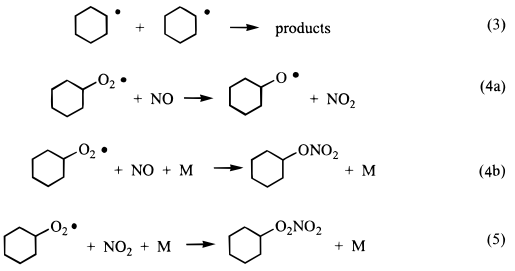

(3)

(4a)

(4b)

(5)

FTIR product studies were performed to determine the fate of the cyclohexoxy radical (c-C_6H_{11})O• formed in reaction 4a.

[†] Current address: Haldor Topsoe A/S, Nymoellevej 55, DK-2800 Lyngby, Denmark. E-mail: jss@topsoe.dk.
[‡] E-mail: ole.john.nielsen@risoe.dk.
[§] E-mail: twalling@ford.com.

10.1021/jp984195x CCC: $18.00
Published on Web 03/11/1999

2. Experimental Section

The two experimental systems used are described in detail elsewhere.[2,3]

2.1. Pulse Radiolysis System. c-C_6H_{11}• radicals were generated from c-C_6H_{12} by the pulsed radiolysis of SF_6/c-C_6H_{12} gasmixtures in a 1 L stainless steel reaction cell with a 30 ns pulse of 2 MeV electrons from a Febetron 705 field emission accelerator. SF_6 was always in great excess and was used to generate fluorine atoms:

$$SF_6 \xrightarrow{2\ \text{MeV}\ e^-} F + \text{products} \qquad (6)$$

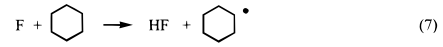

(7)

The radiolysis dose was varied by insertion of stainless steel attenuators between the accelerator and the reaction cell. In this work we refer to the radiolysis dose as a fraction of the maximum dose that is achievable. The fluorine atom yield was calibrated by monitoring the transient absorption at 260 nm by CH_3O_2 radicals produced by pulse radiolysis of $SF_6/CH_4/O_2$ mixtures, as described previously.[4] Using $\sigma(CH_3O_2)_{260\ nm} = 3.18 \times 10^{-18}$ cm^2 molecule^{-1},[5] the F atom yield was determined to be $(3.18 \pm 0.32) \times 10^{15}$ molecules cm^{-3} at full radiolysis dose and 1000 mbar of SF_6 [4]. The quoted error includes 10% uncertainty in $\sigma(CH_3O_2)_{260nm}$ and two standard deviations from the experimental absorption measurements. Unless otherwise stated, all uncertainties reported in this paper are two standard deviations and standard error propagation methods were used.

The analysis light was provided by a pulsed 150 W Xenon arc lamp and was multipassed through the reaction cell using internal White cell optics to give total optical path lengths of 80, 160, or 200 cm. After leaving the cell, the light was guided through a monochromator and detected by a photomultiplier (to record absorption transients) or by a diode array (to record absorption spectra). All absorption transients were derived from single pulse experiments. Using the photomultiplier detector, the spectral resolution was 0.8 nm while it was 1 nm when the diode array was used to record spectra. Spectral calibration was achieved using a Hg pen ray lamp.

Reagent concentrations used were SF_6, 980−995 mbar; c-C_6H_{12}, 5 mbar; O_2, 0.95−15.0 mbar; NO, 0.32−1.16 mbar; and NO_2, 0.34−1.07 mbar. All experiments were performed at 296 ± 2 K and 1000 mbar total pressure. Chemicals were supplied by SF_6 (99.9%), Gerling and Holz; c-C_6H_{12} (>99%) Aldrich; O_2, (ultrahigh purity) L'Air Liquide; NO_2 (>98%), Linde Technische Gase; and NO (99.8%), Messer Griesheim. All chemicals were used as received.

Five sets of experiments were performed using the pulse radiolysis system. First, the UV absorption spectra of c-C_6H_{11}• and (c-C_6H_{11})O_2• radicals were obtained using the diode array camera to capture the UV absorption following radiolysis of SF_6/c-C_6H_{12} and SF_6/c-C_6H_{12}/O_2 mixtures. Second, the rate constant for reaction 3 was determined from the rate of the decay of the absorption at 250 nm, following the radiolysis of SF_6/c-C_6H_{12} mixtures.

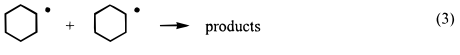

(3)

Third, the rate constant for the association reaction between the c-C_6H_{11}• radical and O_2 was measured by monitoring the formation of (c-C_6H_{11})O_2• radicals in the presence of O_2. Fourth, the rate of NO_2 formation following radiolysis of SF_6/c-C_6H_{12}/O_2/NO mixtures was used to measure the rate constant for the reaction of (c-C_6H_{11})O_2• radicals with NO. Finally, k_5 was determined by monitoring the rate of NO_2 loss following radiolysis of SF_6/c-$C_6H_{12}/O_2/NO_2$ mixtures:

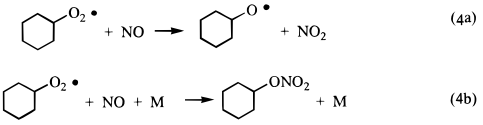

(4a)

(4b)

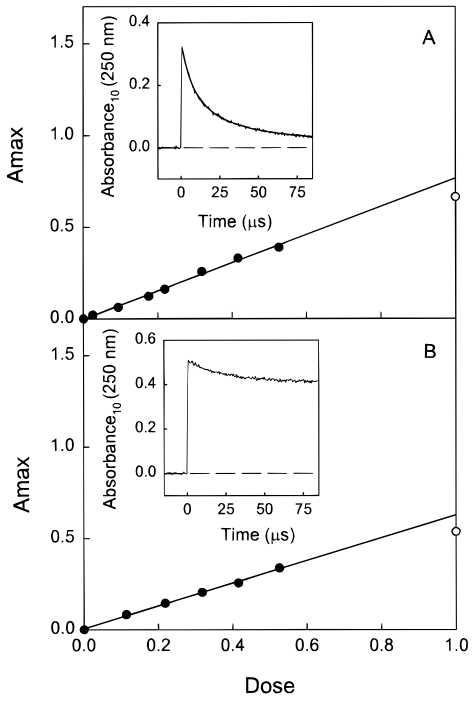

Figure 1. Observed maximum transient absorbance (base 10) at 250 nm versus radiolysis dose following pulsed radiolysis of mixtures of either (A) 5 mbar c-C_6H_{12} and 995 mbar SF_6 or (B) 5 mbar c-C_6H_{12}, 15 mbar O_2, and 980 mbar SF_6. The solid lines are linear regressions of the low dose data (filled circles). The inserts show typical transient absorption traces using (A) 5 mbar c-C_6H_{12} and 995 mbar SF_6, dose = 32% of maximum, UV path length = 80 cm and (B) 5 mbar c-C_6H_{12}, 15 mbar O_2, and 980 mbar SF_6, dose = maximum, UV path length = 80 cm. The smooth line in the insert in part A is a second-order decay fit.

2.2. FTIR−Smog Chamber System. The FTIR system was interfaced to a 140 L Pyrex reactor. Radicals were generated by the UV irradiation (22 blacklamps) of gas mixtures containing 20−96 mTorr of c-C_6H_{12}, 100−250 mTorr of Cl_2, 50−595 Torr of O_2, 50−100 mTorr of NO, and 9.21 mTorr of NO_2 in 700 Torr total pressure with (N_2 + O_2) diluent at 296 ± 2 K (760 Torr = 1013 mbar = 101.3 kPa). Reactant loss and product formation were monitored by FTIR spectroscopy, using an analyzing path length of 27 m and a resolution of 0.25 cm^{-1}. Infrared spectra were derived from 32 coadded spectra. Reference spectra were acquired by expanding known volumes of authentic reference compounds into the chamber.

3. Results and Discussion

3.1. UV Absorption Spectrum of the c-C_6H_{11}• Radical. Following the pulse radiolysis of SF_6/c-C_6H_{12} mixtures, a rapid (complete within 0.5−1.5 μs) increase in absorption was observed at 250 nm, followed by a slower decay. The insert in Figure 1A shows the transient absorption at 250 nm following

the radiolysis of a mixture of 995 mbar SF_6 and 5 mbar c-C_6H_{12}. No absorption was observed when either 995 mbar of SF_6, or 5 mbar of c-C_6H_{12}, were radiolyzed separately. We ascribe the absorption shown in the insert Figure 1A to formation of c-C_6H_{11}• radicals and their subsequent loss by self-reaction. In this work we assume that F atoms react exclusively with c-C_6H_{12} by H atom abstraction to give c-C_6H_{11}• radicals. To work under conditions where 100% of the F atoms are converted into alkyl radicals, it is necessary to consider potential interfering radical−radical reactions such as reactions 3 and 8:

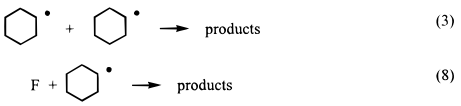

To check for such complications, experiments were performed using mixtures of 995 mbar of SF_6 and 5 mbar of c-C_6H_{12}, with the maximum transient absorption at 250 nm measured as a function of radiolysis dose. Figure 1A shows the observed maximum absorbance as a function of the dose. As seen from Figure 1A, the absorption observed in experiments using maximum dose (open circle) was significantly less than that expected based upon a linear extrapolation of the low dose data (filled circles). This observation suggests that unwanted radical−radical reactions such as reactions 3 and 8 become important at higher radical concentrations.

The line through the experimental data in Figure 1A is a linear least-squares fit to the low dose data and has a slope of 0.769 ± 0.044. Combining this slope with the F atom yield of (3.18 ± 0.32) × 10^{15} molecules cm^{-3} (full dose and $[SF_6] = 1000$ mbar), we obtain σ(c-C_6H_{11}•)$_{250\ m} = (7.00 \pm 0.81) \times 10^{-18}$ cm^2 $molecule^{-1}$. The quoted uncertainty includes both statistical and potential systematic uncertainties and so reflects the accuracy of the measurement.

The spectrum of the c-C_6H_{11}• was measured by recording the initial absorbance following the pulsed radiolysis of SF_6/c-C_6H_{12} mixtures using a diode array. The delay was 0.1 μs, the integration time was 1 μs, and the spectral resolution was 1 nm. The initial absorbances were scaled to that at 250 nm and placed on an absolute basis using σ(c-C_6H_{11}•)$_{250nm} = (7.00 \pm 0.81) \times 10^{-18}$ cm^2 $molecule^{-1}$. The result is shown in Figure 2A. For comparison the UV absorption spectrum of the c-C_6H_{11}• radical reported by Schuler and Patterson[6] is also given in Figure 2A. This spectrum was obtained in liquid cyclohexane and, for reasons which are unknown, is substantially less intense than the gas-phase spectrum reported herein.

3.2. Kinetic Study of the Self-Reaction of c-C_6H_{11}• Radicals. The insert in Figure 1A shows a typical absorption trace obtained by pulse radiolysis of a mixture of 995 mbar SF_6 and 5 mbar c-C_6H_{12}. The trace shows a rapid increase in absorption at 250 nm followed by a slower decay. We ascribe the decay to the self-reaction of the c-C_6H_{11}• radicals, via reaction 3, The

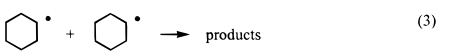

decay was fitted with the second-order decay expression $A(t) = (A_0 - A_{inf})/(1 + 2k_3(A_0 - A_{inf})t) + A_{inf}$, where $A(t)$ is the measured absorbance at time t and A_0 and A_{inf} are the absorbances extrapolated to time zero and infinite time, respectively. The fit is shown in the insert Figure 1A. No residual absorption was observed, indicating the absence of any long-lived products which absorb significantly at 250 nm.

The reciprocal half-lives, $1/t_{1/2}$ (derived from the fits), are plotted as a function of A_0 in Figure 3. The c-C_6H_{11}• concentration was varied by varying the initial F atom concentration. A linear least-squares fit of the data in Figure 3 gives a slope of (2.47 ± 0.05) × 10^5 s^{-1} = (k_3 2 ln 10)/(σ(alkyl)L), where σ(alkyl) is the absorption cross section of the c-C_6H_{11}• radical and L is the optical path length (80 cm). The intercept of the linear regression of the data (0.06 ± 0.08) × 10^5 s^{-1} is not significantly different from zero. The slope of (2.47 ± 0.05) × 10^5 s^{-1} can be combined with σ(c-C_6H_{11}•)$_{250\ nm} = (7.00 \pm 0.81) \times 10^{-18}$ cm^2 $molecule^{-1}$ to give $k_3 = (3.0 \pm 0.4) \times 10^{-11}$ cm^3 $molecule^{-1}$ s^{-1}. The quoted error includes statistical uncertainties associated with both the slope in Figure 3 and σ(c-C_6H_{11}•)$_{250\ nm}$. As expected for such structurally similar radicals, k_3 is indistinguishable from the rate constants for the self-reaction of alkyl radicals derived from 1,4-dioxane and 1,3,5-trioxane, (3.3 ± 0.4) × 10^{-11} and (3.1 ± 0.6) × 10^{-11} cm^3 $molecule^{-1}$

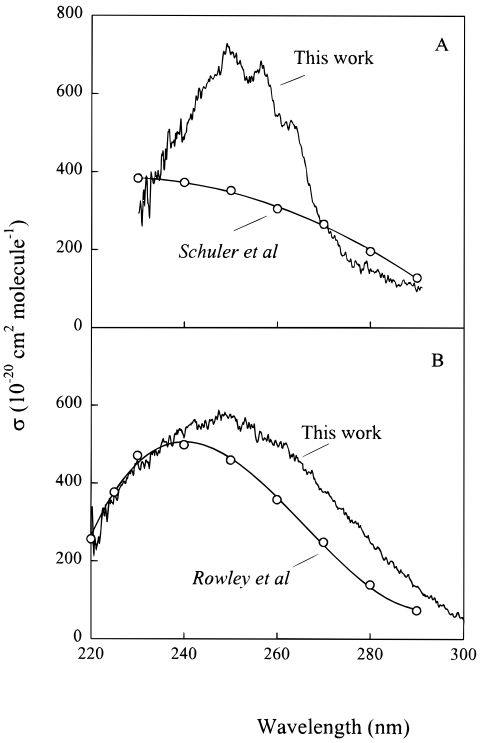

Figure 2. (A) UV-absorption spectrum of the c-C_6H_{11}• radical reported by Schuler and Patterson[6] (circles) and measured herein (solid line). (B) UV-absorption spectrum of the (c-C_6H_{11})O_2• radical reported by Rowley et al.[13] (circles) and measured in the present work (solid line).

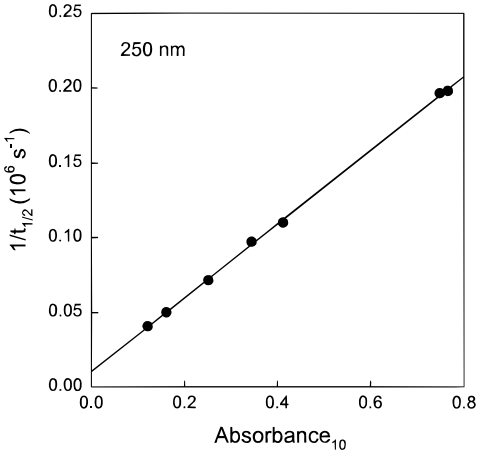

Figure 3. Plot of the reciprocal half-life for self-reaction of c-C_6H_{11}• radicals as a function of the maximum absorbance at 250 nm.

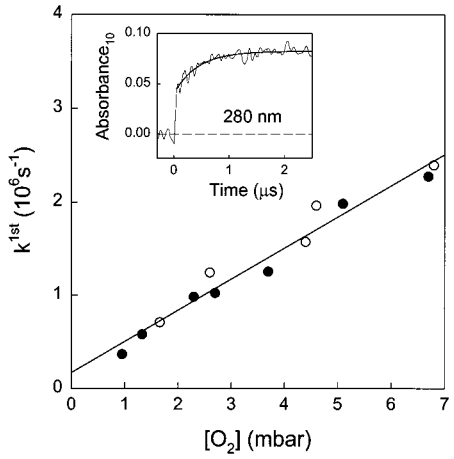

Figure 4. Pseudo-first-order rate constants for the formation of (c-C_6H_{11})O_2• radicals as a function of the O_2 concentration in 500 (opened circles) and 1000 (filled circles) mbar of SF_6, diluent. The insert shows an experimental transient obtained using a mixture of 5 mbar c-C_6H_{12}, 5.1 mbar O_2, and 990 mbar SF_6. The UV path length was 80 cm and the radiolysis dose was 32% of maximum. The smooth curve in the insert is the first-order fit (starting at $t = 0.2$ μs).

s^{-1}.[7,8] The kinetics of reaction 3 have been studied previously by Schuler and Patterson.[6] For reasons which are unknown, the value of k_3 reported by Schuler and Patterson[6] is a factor of 16 times less than that reported herein.

3.3. Association Reaction between O_2 and c-C_6H_{11}• Radicals. The kinetics of reaction 2 were studied by monitoring the absorbance at 280 nm following pulse radiolysis of mixtures of 495−995 mbar of SF_6, 5.0 mbar of c-C_6H_{12}, and 0.95−6.8 mbar of O_2. Assuming k_7 to be approximately 1×10^{-10} cm^3 $molecule^{-1}$ s^{-1},[9] it follows that in the presence of 5.0 mbar of c-C_6H_{12} the lifetime of F atoms with respect to conversion into c-C_6H_{11}• radicals is 0.08 μs. Assuming that c-C_6H_{11}• radicals behave like other alkyl radicals and add O_2 with a rate constant of the order 10^{-12}−10^{-11} cm^3 $molecule^{-1}$ s^{-1}, the lifetime of c-C_6H_{11}• radicals with respect to conversion into (c-C_6H_{11})O_2• radicals will be of the order of a microsecond. Consistent with expectations, the pulsed radiolysis of SF_6/c-C_6H_{12}/O_2 mixtures produced absorption transients consisting of a initial rapid increase in absorption (complete within 0.1 μs) followed by a slower increase which occurred over a time scale of 1−4 μs. We ascribe the initial rapid increase in absorption to the rapid formation of c-C_6H_{11}• radicals and the subsequent "slow" increase to their conversion into (c-C_6H_{11})O_2• radicals. The "slow" increase in absorption was observed to follow first-order kinetics. The insert in Figure 4 shows a typical absorption transient together with a first-order fit. As seen from Figure 4, the pseudo-first-order rate constant k^{first} increased linearly with O_2 concentration. Experiments were performed in the presence of either 500 or 1000 mbar total pressure using SF_6 as diluent; there was no discernible effect of total pressure suggesting that reaction 2 is at, or near, the high-pressure limit in 500−1000 mbar of SF_6. This behavior is consistent with the available database for the addition of O_2 to large ($\geq C_3$) alkyl radicals.[9] Linear least-squares analysis of the data in Figure 4 gives $k_2 = (1.3 \pm 0.2) \times 10^{-11}$ cm^3 $molecule^{-1}$ s^{-1}. This result is in excellent agreement with that of $k_2 = (1.4 \pm 0.2) \times 10^{-11}$ cm^3 $molecule^{-1}$ s^{-1} measured by Wu et al.[10] in a previous gas phase study. In contrast, a value of $(5.6 \pm 1.0) \times 10^{-12}$ cm^3 $molecule^{-1}$ s^{-1} has been measured in liquid cyclohexane by Bjellqvist and Reitberger.[11]

3.4. Spectrum of (c-C_6H_{11})O_2• Radicals. Following the pulse radiolysis of mixtures of 980 mbar SF_6, 5 mbar c-C_6H_{12}, and 15 mbar O_2, a rapid increase (complete within 0.5−2.0 μs) in the UV absorbance was observed, followed by a slower decay. An example is shown in the insert in Figure 1B. The observed absorption does not decay to zero, indicating the formation of a reaction product which absorbs at 250 nm. We ascribe the initial increase in absorption to the formation of the (c-C_6H_{11})-O_2• via reaction 2. To work under conditions where a known fraction of the F atoms are converted into (c-C_6H_{11})O_2• radicals, it is necessary to consider potential interfering secondary chemistry. Potential complications include unwanted radical−radical reactions such as reactions 3 and 8−10.

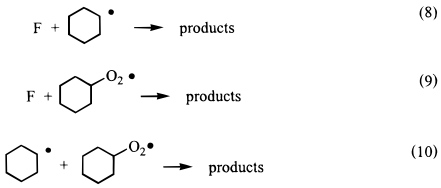

and loss of F atoms by reaction with molecular oxygen, reaction 11:

$$F + O_2 + M \rightarrow FO_2 + M \qquad (11)$$

Assuming $k_7 = 1 \times 10^{-10}$ cm^3 $molecule^{-1}$ s^{-1} [9] and using $k_{13} = (1.9 \pm 0.3) \times 10^{-13}$ cm^3 $molecule^{-1}$ s^{-1},[12] we calculate that 0.6% of the F atoms are converted into FO_2 radicals and 99.4% into (c-C_6H_{11})O_2• radicals. No corrections due to formation of FO_2 radicals was necessary.

There are no literature data concerning the kinetics of reactions 8−10, hence, we cannot calculate their importance. To check for these unwanted radical−radical reactions, the transient absorbance at 250 nm was measured using mixtures of 980 mbar SF_6, 5 mbar c-C_6H_{12}, and 15 mbar O_2 with the radiolysis dose varied by an order of magnitude. The UV path length was 80 cm. Figure 1B shows the observed maximum absorbance of the experimental transients at 250 nm as a function of dose. As seen from Figure 1B, the absorption observed in experiments using maximum dose (open circle) was significantly less than that expected upon linear extrapolation of the low dose data (filled circles). We ascribe this to incomplete conversion of F atoms into (c-C_6H_{11})O_2• radicals caused by secondary radical−radical reactions 3 and 8−10 at high radical concentrations. The solid line drawn through the data in Figure 1B is a linear least-squares fit of the low dose data. The slope is 0.62 ± 0.03. From this value and the yield of F atoms of $(3.18 \pm 0.32) \times 10^{15}$ molecule cm^{-3} (full dose and $[SF_6] = 1000$ mbar), we derive $\sigma((c\text{-}C_6H_{11})O_2\bullet)_{250nm} = (5.72 \pm 0.64) \times 10^{-18}$ cm^2 $molecule^{-1}$. The quoted uncertainty includes both statistical and potential systematic uncertainties and so reflects the accuracy of the measurement.

To map out the spectrum of the (c-C_6H_{11})O_2• radical, the maximum transient absorbance between 220 and 300 nm following the pulsed radiolysis of SF_6/c-C_6H_{12}/O_2 mixtures was recorded using a diode array. The delay was 0.1 μs, the integration time was 1 μs, and the spectral resolution was 1 nm. The initial absorbances were scaled to that at 250 nm and placed on an absolute basis using $\sigma((c\text{-}C_6H_{11})O_2\bullet) = 5.72 \times 10^{-18}$ cm^2 $molecule^{-1}$. The result is shown in Figure 2B. The UV spectrum of (c-C_6H_{11})O_2• radicals reported by Rowley et al.[13] is also given in Figure 2B. For reasons which are unclear, the spectrum measured in the present study is slightly (10%)

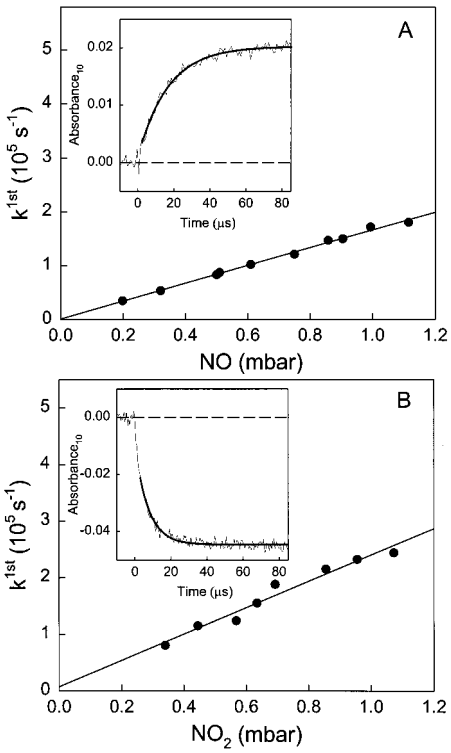

Figure 5. (A) Pseudo-first-order rate constants for formation of NO_2 following pulsed radiolysis of SF_6/cyclohexane/O_2/NO mixtures versus [NO]. The insert shows the transient absorbance at 400 nm observed following pulsed radiolysis of a mixture of 0.40 mbar NO, 10 mbar cyclohexane, 10 mbar O_2, and 980 mbar SF_6. (B) Pseudo-first-order rate constants for decay of NO_2 following pulsed radiolysis of SF_6/cyclohexane/O_2/NO_2 mixtures versus [NO_2]. The insert shows the transient absorbance at 400 nm observed following pulsed radiolysis of a mixture of 0.64 mbar NO_2, 10 mbar cyclohexane, 10 mbar O_2, and 980 mbar SF_6.

less intense and is shifted to the red by approximately 10 nm when compared to that of Rowley et al.[13]

3.5. Kinetics of the Reaction between (c-C_6H_{11})O_2• Radicals and NO. The kinetics of reaction 4 were studied by monitoring the increase in absorption at 400 nm, ascribed to the formation of NO_2, following the pulse radiolysis of c-C_6H_{12}/O_2/NO/SF_6 mixtures. The initial conditions were 10 mbar c-C_6H_{12}, 10 mbar O_2, 0.34−1.16 mbar NO, in 1000 mbar of SF_6 diluent. The insert in Figure 5A shows a typical absorption transient observed following the pulsed radiolysis of a mixture containing 0.40 mbar of NO.

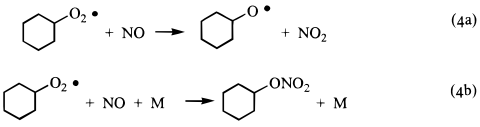

The absorption transients were fitted using a first-order kinetic expression, and the resulting pseudo-first-order rate constants are plotted versus the initial NO concentration in Figure 5A. This method of measuring the kinetics of the reactions of alkyl peroxy radicals with NO has been used previously in our laboratory and is discussed in detail elsewhere.[14] As seen from Figure 5A, the pseudo-first-order rate constants k^{first} increased linearly with the NO concentration. Linear least-squares analysis of the data in Figure 5A gives $k_4 = (6.7 \pm 0.9) \times 10^{-12}$ cm^3 molecule^{-1} s^{-1}. The NO_2 yield calculated from the observed maximum absorbance was 86 ± 10% of that expected if all F atoms were converted into (c-C_6H_{11})O_2• radicals and all the (c-C_6H_{11})O_2• radicals reacted via reaction 4a, which we ascribe to a minor contribution from reaction channel 4b.

3.6. Kinetics of the Reaction between (c-C_6H_{11})O_2• Radicals and NO_2. The kinetics of reaction 5 were studied by monitoring the decrease in absorbance at 400 nm following the pulsed radiolysis of mixtures of 10 mbar c-C_6H_{12}, 10 mbar O_2, 0.34−1.07 mbar NO_2, and SF_6 added to 1000 mbar total pressure. The insert in Figure 5B shows the absorbance as a function of time after the radiolysis of a mixture containing 0.64 mbar of NO_2. The rate of decay of the absorbance at 400 nm increased linearly with the NO_2 concentration. We ascribe the decrease in absorbance to loss of NO_2 in the system. Three reactions could be responsible for the NO_2 loss:

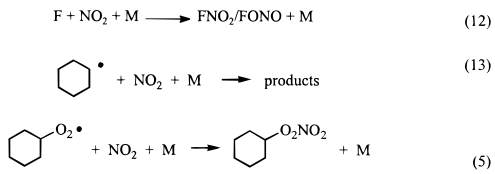

However, the time scale of the decay shown in the insert (Figure 5B) is only consistent with reaction 5 causing the loss of NO_2 (the lifetimes of both F atoms and c-C_6H_{11}• radicals are <1 μs, see section 3.3).

The smooth curve in the insert (Figure 5B) is the first-order fit which gives a pseudo-first-order rate constant, $k^{first} = 1.55 \times 10^5$ s^{-1}. To allow sufficient time for conversion of F atoms into the alkyl peroxy radicals the analysis of the decay traces was performed starting 2 μs after the radiolysis pulse. k^{first} values for eight experiments with different concentrations of NO_2 are shown in Figure 5B. Linear least-squares analysis of the data in Figure 5B gives $k_5 = (9.5 \pm 1.5) \times 10^{-12}$ cm^3 molecule^{-1} s^{-1}. The observed loss of NO_2 was 88 ± 10% of the initial concentration of (c-C_6H_{11})O_2• radicals.

3.7. IR Absorption Spectrum of (c-C_6H_{11})O_2NO_2. Prior to our study of the atmospheric oxidation mechanism of cyclohexane in the presence of NO_x, the IR spectrum of the peroxynitrate, (c-C_6H_{11})O_2NO_2, was recorded using the FTIR−smog chamber system. (c-C_6H_{11})O_2NO_2 was prepared by the UV irradiation of a mixture of 34.7 mTorr c-C_6H_{12}, 9.21 mTorr NO_2, and 167 mTorr Cl_2 in 700 Torr total pressure of O_2 diluent. Twenty seconds of UV irradiation resulted in the consumption of 16% of the cyclohexane and the formation of product features at 791, 919, 1042, 1295, 1457, and 1715 cm^{-1}. Figure 6 shows the product spectrum obtained after subtraction of features attributable to cyclohexane which we assign to (c-C_6H_{11})O_2NO_2 formed in the following reactions:

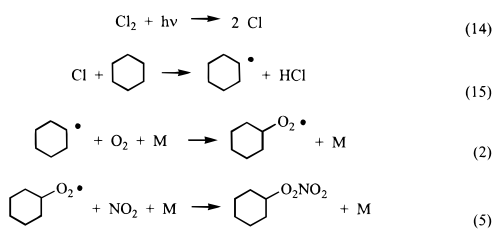

The *y*-axis scale in Figure 6 was placed upon an absolute basis by equating the observed loss of cyclohexane to formation of peroxynitrate. NO_2 absorbs strongly in the region 1500−1660 cm^{-1}, and we are unable to provide spectral information for (c-C_6H_{11})O_2NO_2 in this region. The IR feature at 1295 cm^{-1}

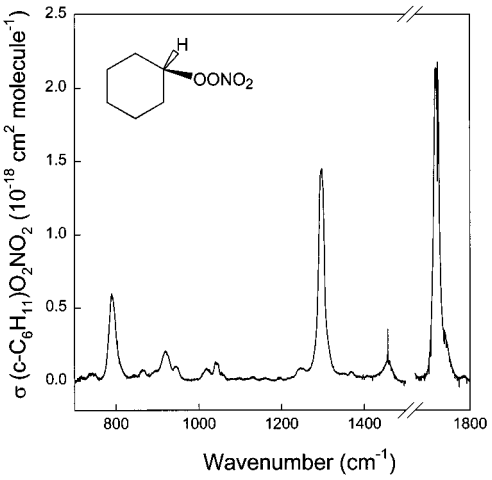

Figure 6. IR spectrum of peroxynitrate (c-C_6H_{11})O_2NO_2.

is assigned to the NO_2 symmetric stretching mode which is a characteristic feature in the IR spectra of organic nitrates. The integrated absorption cross section of this band is 2.48×10^{-17} cm molecule^{-1} and is comparable to those reported for the analogous features in CH_3ONO_2 (2.90×10^{-17} [15]), $C_2H_5ONO_2$ (2.97×10^{-17} [15]), and $CH_3C(O)O_2NO_2$ (2.58×10^{-17} [15]) providing confidence that the spectrum shown in Figure 6 is indeed that of (c-C_6H_{11})O_2NO_2.

3.8. Nitrate Yield in the (c-C_6H_{11})O_2• + NO Reaction and Rate Constant Ratio k_{17}/k_{16}. To determine the branching ratio $k_{4b}/(k_{4a} + k_{4b})$ and the rate constant ratio k_{17}/k_{16}, the FTIR−smog chamber system was used to study the products resulting from the Cl atom initiated oxidation of cyclohexane in the presence of NO. Experiments were conducted using c-C_6H_{12}/NO/Cl_2/O_2/N_2 mixtures in 700 Torr total pressure at 296 ± 2 K.

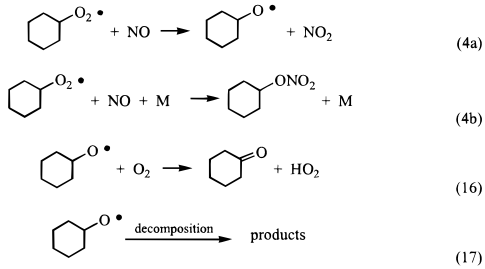

Cyclohexane loss and product formation were monitored using FTIR spectroscopy. Figure 7 shows IR spectra acquired before (A) and after (B) a 90 s irradiation of a mixture of 19.6 mTorr c-C_6H_{12}, 90 mTorr Cl_2, 46 mTorr NO, and 595 Torr O_2 in 700 Torr total pressure with N_2 diluent. Part C shows a reference spectrum of cyclohexanone. Comparison of part B with part C shows that cyclohexanone is a significant product. The infrared features at 1121 and 1221 cm^{-1} were used to quantify the cyclohexanone yield. Experiments were performed using $[O_2] = 50-595$ Torr. The cyclohexanone yield increased with increasing $[O_2]$ reflecting a competition between reactions 16 and 17 for the available cyclohexoxy radicals produced in reaction 4a. Subtraction of features attributable to c-C_6H_{12}, cyclohexanone, HONO, HNO_3, and c-$C_6H_{11}O_2NO_2$ from part B gives the residual spectrum shown in part D which has a prominent feature at 1281 cm^{-1} characteristic of an organic nitrate. Several nitrates could be responsible for the 1281 cm^{-1} feature in part D; the possibilities include: c-$C_6H_{11}ONO_2$ from reaction 4b and $HC(O)(CH_2)_4CH_2ONO_2$ from a reaction analogous to reaction 4b involving the peroxy radical derived from the alkyl radical generated in reaction 17. For the experiment shown in Figure 7 ($[O_2] = 595$ Torr), the cyclohexanone yield is 70%, the dominant fate of cyclohexoxy radicals is reaction with O_2 and complications caused by nitrates formed after decomposition of cyclohexoxy radicals should be of minor importance. The c-$C_6H_{11}ONO_2$ yield was estimated using an integrated absorption cross section for the IR band centered at 1281 cm^{-1} of 2.7×10^{-17} cm molecule^{-1} (average of values listed in previous section for organic nitrates). Figure 8 shows c-$C_6H_{11}ONO_2$ formation versus c-C_6H_{12} loss (corrected for the formation of a small amount of c-$C_6H_{11}O_2NO_2$ via reaction 5) from experiments conducted using $[O_2] = 595$ Torr. Linear least-squares regression of the data in Figure 8 gives $k_{4b}/(k_{4a} + k_{4b}) = 0.197 \pm 0.010$. Incorporating an estimated uncertainty of 15% in the integrated cross section of 2.7×10^{-17} gives $k_{4b}/(k_{4a} + k_{4b}) = 0.197 \pm 0.031$. It should be noted that this approach overestimates the branching ratio because of the possible contribution of nitrates formed after decomposition of the cyclohexoxy radicals via reaction 17. This point is addressed at the end of this section.

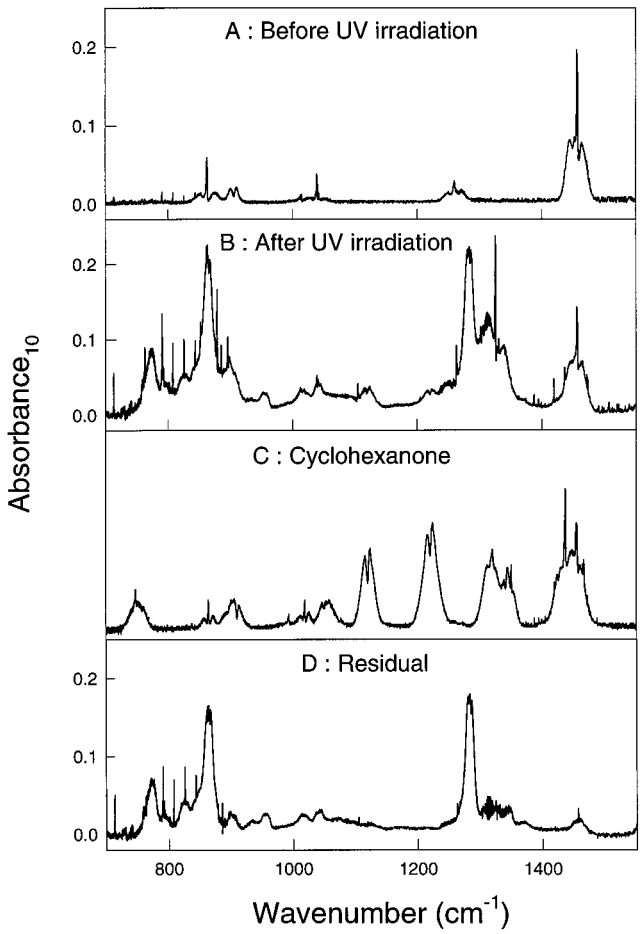

Figure 7. IR spectra acquired before (A) and after (B) a 90 s irradiation of a mixture of 19.6 mTorr c-C_6H_{12}, 90 mTorr Cl_2, 46 mTorr NO, and 595 Torr O_2 in 700 Torr total pressure of N_2 diluent. During the irradiation 47% of the c-C_6H_{12} was consumed. Part C shows a spectrum of cyclohexanone. Subtraction of IR features attributable to c-C_6H_{12}, cyclohexanone, HONO, HNO_3, and (c-C_6H_{11})-O_2NO_2 from part B gives part D. The prominent feature at 1281 cm^{-1} is a typical IR feature of an organic nitrate (see text for details).

Reactions 16 and 17 compete for the cyclohexoxy radicals produced in reaction 4a. If we define α as the yield of cyclohexoxy radicals from reaction 4, $\alpha = k_{4a}/(k_{4a} + k_{4b})$,

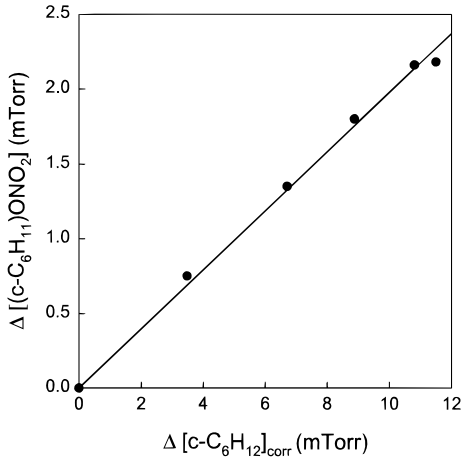

Figure 8. Yield of $(c\text{-}C_6H_{11})ONO_2$ following the UV irradiation $c\text{-}C_6H_{12}/Cl_2/NO/O_2/N_2$ mixtures as a function of the $c\text{-}C_6H_{12}$ loss (corrected for formation of $(c\text{-}C_6H_{11})O_2NO_2$) at constant total pressure (700 or 750 Torr) and 296 ± 2K. The fit through the data is a linear least squares regression which gives a $(c\text{-}C_6H_{11})ONO_2$ yield of 19.7 ± 0.1%.

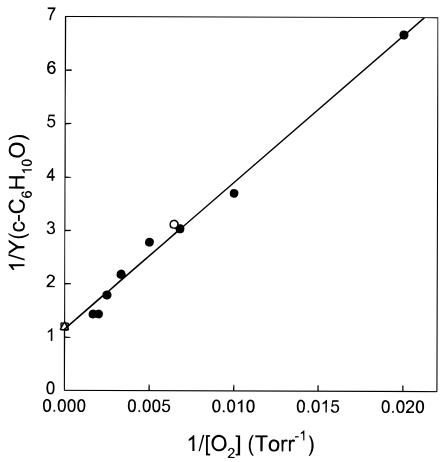

Figure 9. Reciprocal yield of cyclohexanone following the UV irradiation of $c\text{-}C_6H_{12}/Cl_2/NO/O_2/N_2$ mixtures as a function of the reciprocal oxygen concentration at a total pressure of 700 or 750 Torr and 296 ± 2K. Closed circles are data obtained in this work; the open circle is taken from Aschmann et al.[18] The open triangle and square are the limiting cases calculated using a $(c\text{-}C_6H_{11})ONO_2$ yield of 0.16 (this work) and 0.156 (Aschmann et al.[18] (see text for details).

then the molar yield of cyclohexanone $Y(c\text{-}C_6H_{10}O)$ can be expressed as

$$Y(c\text{-}C_6H_{10}O) = \alpha\left(\frac{k_{16}[O_2]}{(k_{16}[O_2] + k_{17})}\right)$$

and

$$\frac{1}{Y(c\text{-}C_6H_{10}O)} = \frac{1}{\alpha}\frac{k_{17}}{k_{16}}\frac{1}{[O_2]} + \frac{1}{\alpha}$$

where k_{16} and k_{17} are rate constants for reactions 16 and 17. The yield of cyclohexanone was measured in experiments conducted using the UV irradiation of $c\text{-}C_6H_{12}/NO/Cl_2/O_2/N_2$ mixtures with $[O_2]$ varied between 50 and 595 Torr. For each experiment the cyclohexanone yield was obtained from a linear least squares regression of a plot of cyclohexanone formation versus $c\text{-}C_6H_{12}$ consumption. The rate constant for the reaction between Cl atoms and cyclohexanone is 3.4×10^{-10} cm^3 molecule^{-1} s^{-1}.[16] Small corrections (4−25%) were applied to account for loss of cyclohexanone via reaction with Cl atoms using methods described previously.[17]

Figure 9 shows a plot of $1/Y(c\text{-}C_6H_{10}O)$ versus $1/[O_2]$. The filled circles in Figure 9 are results from the present work, the open circle is the cyclohexanone yield observed during cyclohexane oxidation in air reported by Atkinson et al.[18] The fit shown in Figure 9 is a linear regression to both data sets giving an intercept of $1/\alpha = 1.11 \pm 0.15$ and a slope of $(1/\alpha)x(k_{17}/k_{16}) = 279 \pm 20$ Torr; hence, $k_{17}/k_{16} = 251 \pm 47$ Torr. Quoted errors in k_{17}/k_{16} include uncertainties in both the slope and intercept. There are no literature data to compare with this result.

At this point, it is appropriate to return to the estimation of $k_{4b}/(k_{4a} + k_{4b}) = 0.197 \pm 0.043$ above and consider the likely impact of the formation of nitrates formed after decomposition of the cyclohexoxy radicals. Using $k_{17}/k_{16} = 251$ Torr it follows that, in the presence of 595 Torr of O_2, 30% of the cyclohexoxy radicals will decompose via reaction 17 while the remaining 70% will react with O_2. On the basis of the literature database for hexyl and pentyl peroxy radicals,[19] it is likely that 10−20% of the peroxy radicals formed following reaction 17 will react with NO to give nitrates. Correcting for the formation of such nitrates we arrive at $k_{4b}/(k_{4a} + k_{4b}) = 0.16 \pm 0.04$, where the quoted error includes uncertainties associated with the correction procedure. This result is in good agreement with the value of $k_{4b}/(k_{4a} + k_{4b}) = 0.156 \pm 0.017$ reported by Aschmann et al.[18] but somewhat higher than that of $k_{4b}/(k_{4a} + k_{4b}) = 0.09 \pm 0.04$ reported by Tagagi et al.[20] The open triangle and square in Figure 9 are the limiting cases calculated using values of $k_{4b}/(k_{4a} + k_{4b}) = 0.16$ (derived above) and 0.156[18] and are consistent with expectations based upon extrapolation of cyclohexanone yields observed using experiments with $[O_2] = 50-592$ Torr.

4. Discussion

The results presented here improve our understanding of the atmospheric degradation mechanism of cyclohexane. Oxidation is initiated via OH radical attack which occurs with a rate constant of 7.4×10^{-12} cm^3 molecule^{-1} s^{-1} at 298 K.[21] While the concentration of OH radicals in the atmosphere varies considerably both spatially and temporally, a reasonable estimate of the 24 h average OH radical concentration is $0.5-1.0 \times 10^6$ cm^{-3}. Hence, the atmospheric lifetime of cyclohexane lies in the range 1−3 days. Reaction of OH radicals with cyclohexane gives cyclohexyl radicals, $c\text{-}C_6H_{11}^{\bullet}$, which add O_2 with a rate constant $k_2 = (1.3 \pm 0.2) \times 10^{-11}$ cm^3 molecule^{-1} s^{-1}. In 1 atm of air at 298 K, the lifetime of $c\text{-}C_6H_{11}^{\bullet}$ radicals with respect to addition of O_2 is 15 ns. The sole atmospheric fate of $c\text{-}C_6H_{11}^{\bullet}$ is addition of O_2 to give $c\text{-}C_6H_{11}O_2^{\bullet}$ radicals.

We have shown here that $c\text{-}C_6H_{11}O_2^{\bullet}$ radicals react with NO giving a (16 ± 4)% yield of the nitrate $(c\text{-}C_6H_{11})ONO_2$ with the balance of reaction producing $c\text{-}C_6H_{11}O$ radicals and NO_2. Using $k_4 = (6.7 \pm 0.9) \times 10^{-12}$ cm^3 molecule^{-1} s^{-1}, together with an estimated background tropospheric NO concentration of 2.5×10^8 molecule cm^{-3} [22], gives a lifetime of $c\text{-}C_6H_{11}O_2^{\bullet}$ radicals with respect to reaction with NO of 10 min. $c\text{-}C_6H_{11}O_2^{\bullet}$ radicals also react rapidly with NO_2, but the peroxynitrate product is thermally unstable and decomposes to regenerate $c\text{-}C_6H_{11}O_2^{\bullet}$ radicals and NO_2[19] and therefore is not an important atmospheric oxidation product. Reaction with O_2 and ring opening via C−C bond scission are two competing atmospheric fates of the $c\text{-}C_6H_{11}O^{\bullet}$ radical produced in the $c\text{-}C_6H_{11}O_2^{\bullet}$ + NO reaction. In 700−750 Torr total pressure at 296 ± 2K the rate constant ratio $k_{decomp}/k_{O2} = (8.1 \pm 1.5) \times 10^{18}$ molecule cm^{-3}. At 296 K in 1 atm of air, 61% of cyclohexoxy radicals

decompose and 39% react with O_2 to give cyclohexanone. Decomposition produces an alkyl radical which adds O_2 to give the peroxy radical $HC(O)(CH_2)_5O_2$. Aschmann et al.[18] have shown that the reaction of this peroxy radical with NO leads to a variety of different products including the nitrate $HC(O)(CH_2)_5ONO_2$, the dialdehyde $HC(O)(CH_2)_4C(O)H$, and the hydroxydialdehyde $HC(O)CH_2CH(OH)CH_2CH_2C(O)H$. At the present time the absolute yields of these compounds are not known. The rate constant ratio $k_{decomp}/k_{O2} = (8.1 \pm 1.5) \times 10^{18}$ molecule cm^{-3} was measured at $T = 296 \pm 2$K. At the lower temperatures characteristic of the upper troposphere the rates of both reactions 16 and 17 will decrease substantially. Reaction 17 is a unimolecular decomposition and it is expected that k_{17} will be more sensitive than k_{16} to temperature and that the rate constant ratio k_{decomp}/k_{O2} (k_{17}/k_{16}) will decrease with temperature. Hence, the yield of cyclohexanone during the atmospheric oxidation of cyclohexane is expected to increase significantly with altitude. A study of the temperature dependence of k_{decomp}/k_{O2} is beyond the scope of the present work but is clearly needed to better define the atmospheric chemistry of cyclohexane.

At this point it is germane to note that it has been reported recently that chemical activation can play an important role in the atmospheric fate of alkoxy radicals formed via reaction of peroxy radicals with NO.[23−26] In systems where chemical activation is important, plots of carbonyl yield versus $[O_2]$ (e.g., Figure 9) display *y*-axis intercepts which are substantially in excess of unity.[23,26] There is no evidence from the present work that chemical activation plays any role in the fate of c-$C_6H_{11}O^{\bullet}$ radicals.

Acknowledgment. The work at Risø was supported by Ford Forschungzentrum, Aachen.

References and Notes

(1) Siegl, W. O. 1998. Private communication.

(2) Hansen, K. B.; Wilbrandt, R.; Pagsberg, P. *Rev. Sci. Instrum.* **1979**, *50*, 1532.

(3) Wallington, T. J.; Japar, S. M. *J. Atmos. Chem.* **1989**, *9*, 399.

(4) Bilde, M.; Møgelberg, T. E.; Sehested, J.; Nielsen, O. J.; Wallington, T. J.; Hurley, M. D.; Japar, S. M.; Dill, M.; Orkin, V. L.; Buckley, T. J.; Huie, R. E.; Kurylo, M. J. *J. Phys. Chem.* **1996**, *19*, 3514.

(5) Wallington, T. J.; Dagaut, P.; Kurylo, M. J. *Chem. Rev.* **1992**, *92*, 667.

(6) Schuler, R H.; Patterson, L. K. *Chem. Phys. Lett*. **1974**, *27*, 369.

(7) Platz, J.; Sehested, J.; Møgelberg, T. E.; Nielsen, O. J.; Wallington, T. J. *J. Chem. Soc., Faraday Trans.* **1997**, 93, 2855.

(8) Platz, J.; Christensen, L. K.; Sehested, J.; Nielsen, O. J.; Wallington, T. J.; Sauer, C.; Barnes, I.; Becker, K. H.; Vogt, R. *J. Phys. Chem. A* **1998**, *102*, 4829.

(9) Mallard, W. G.; Westley, F.; Herron, J. T.; Hampson, R. F. *NIST Chemical Kinetics Database*, Version 6.0; NIST Standard Reference Data, Gaithersburg, MD, 1994.

(10) Wu, D.; Bayes, K. D. *Int. J. Chem. Kinet*. **1986**, *18*, 547.

(11) Bjellqvist, B.; Reitberger, T.; K. Tek. Hoegsk. *Nucl. Sci. Abstr*. **1974**, *30*, 120.

(12) Ellermann, T.; Sehested, J.; Nielsen, O. J.; Pagsberg, P.; Wallington, T. J. *Chem. Phys. Lett.* **1994**, *218*, 287.

(13) Rowley, D. M.; Lightfoot, P. D.; Lesclaux, R.; Wallington, T. J. *J. Chem. Soc., Faraday Trans*. **1991**, *87*, 3221.

(14) Sehested, J.; Nielsen, O. J.; Wallington, T. J. *Chem. Phys. Lett.* **1993**, *213*, 257.

(15) Tuazon, E. C.; Atkinson, R., *Int. J. Chem. Kinet*. **1990**, 22, 1221.

(16) Wallington, T. J.; Guschin, A.; Hurley, M. D. *Int. J. Chem. Kinet*. **1998**, *30*, 309.

(17) Meagher, R. J.; Mcintosh, M. E.; Hurley, M. D.; Wallington, T. J. *Int. J. Chem. Kinet*. **1997**, *29*, 619.

(18) Aschmann, S. A.; Chew, A. A.; Arey, J.; Atkinson, R. *J. Phys. Chem. A* **1997**, *101*, 8042.

(19) Lightfoot, P. D.; Cox, R. A.; Crowley, J. N.; Destriau, M.; Hayman, G. D.; Jenkin, M. E.; Moortgat, G. K.; Zabel, F. *Atmos. Environ.* **1992**, *26*, 1805.

(20) Takagi, H.; Washida, N.; Bandow, H.; Akimoto, H.; Okuda, M. *J. Phys. Chem*. **1981**, *85*, 2701.

(21) Atkinson, R.; Aschmann, S. M. *Int. J. Chem. Kinet*. **1989**, *21*, 355.

(22) Atkinson, R. Scientific assessment of stratospheric ozone. World Meteorological Organization Global Ozone Research and Monitoring Project, Report No. 20; World Meteorological Organization: Geneva, 1989; Vol. 2, p 167.

(23) Wallington, T. J.; Hurley, M. D.; Fracheboud, J. M.; Orlando, J. J.; Tyndall, G. S.; Sehested, J.; Møgelberg, T. E.; Nielsen, O. J. *J. Phys. Chem.* **1996**, *100*, 18116.

(24) Møgelberg, T. E.; Sehested, J.; Tyndall, G. S.; Orlando, J. J.; Fracheboud, J. M.; Wallington, T. J. *J. Phys. Chem.* **1997**, *101*, 2828.

(25) Bilde, M.; Wallington, T. J.; Ferronato, C.; Orlando, J. J.; Tyndall, G. S.; Estupiñan, E.; Haberkorn, S. *J. Phys. Chem.* **1998**, *102*, 1976.

(26) Orlando, J. J.; Tyndall, G. S.; Bilde, M.; Ferronato, C.; Wallington, T. J.; Vereecken, L.; Peeters. J. *J. Phys. Chem. A* **1998**, *102*, 8116.